NUREG/CR-0838

STABILITY ANALYSIS OF CIRCUMFERENTIAL CRACKS IN REACTOR PIPING SYSTEMS

H. Tada*   P. Paris*
R. Gamble

*Washington University

Steve Scott
Lan-1220

Prepared for
U. S. Nuclear Regulatory Commission

7908070659

585 288

550 327

583 289

Available from
National Technical Information Service
Springfield, Virginia 22161

~~558 326~~

NUREG/CR-0838
R1, R5

STABILITY ANALYSIS OF CIRCUMFERENTIAL CRACKS IN REACTOR PIPING SYSTEMS

H. Tada*   P. Paris*
R. Gamble**

*Center for Fracture Mechanics
Washington University
St. Louis, MO 63130

Manuscript Completed: February 1979
Date Published: June 1979

Prepared for
**Office of Nuclear Reactor Regulation
U. S. Nuclear Regulatory Commission
Washington, D.C. 20555
Under Contract No. NRC-03-78-135

583 290
~~550 329~~

ABSTRACT

A simplified fracture mechanics analysis was performed to determine the potential unstable tearing in boiling water reactor (BWR) stainless steel piping that have severe intergranular stress corrosion cracking (IGSCC). The fracture analysis was based on the tearing stability concept and associated tearing modulus stability criterion.

The results from this study indicate that unstable crack extension would probably not occur in BWR stainless steel piping systems designed in accordance with the ASME Code even though severe IGSCC may be present. The analysis indicated that stainless steel piping with severe IGSCC could experience unstable fracture if the piping length to radius ratio (L/R) was very large (approximately 200). Since the values of L/R for BWR stainless steel piping systems are generally an order of magnitude less than this, large margins against unstable fracture are assured for these systems.

583 291

~~550~~ 330

CONTENTS

Page

ABSTRACT iii
ACKNOWLEDGMENT vii

1.0 INTRODUCTION 1
2.0 METHOD OF ANALYSIS 3

2.1 Location of the Neutral Axis 9
2.2 Plastic Limit Moment 9
2.3 Expression of J 10

3.0 SIMPLIFIED INSTABILITY ANALYSIS 17
4.0 APPLICATION 26
5.0 SUMMARY 29
6.0 REFERENCES 30

583 292

~~550 331~~

LIST OF FIGURES

Figure	Title	Page
1	Limit moment, M_p, and angle of rotation, ϕ	5
2	Cracked section of pipe	6
3	Location of neutral axis, α	8
4	M_p versus θ, without crack closure	11
5	M_p versus θ, with crack closure	12
6	F_J versus θ, without crack closure	14
7	F_J versus θ, with crack closure	15
8	Cracked beam with arbitrary cross section	16
9	Fixed beam under uniform bending, $\tilde{\phi}$ = constant	18
10	F_1 versus θ, without crack closure	22
11	F_1 versus θ, with crack closure	23
12	F_2 versus θ, without crack closure	24
13	F_2 versus θ, with crack closure	25
14	Simply supported beams, Δ = constant	27

583 293

~~550 332~~

ACKNOWLEDGMENT

The authors ackowledge the support of this work by the U.S. Nuclear Regulatory Commission, Contract Number NRC-03-78-135, and by Washington University, St. Louis, Missouri. The encouragement of the Regulatory staff, especially that of Dr. R. E. Johnson, is gratefully acknowledged.

583 294

~~550 333~~

STABILITY ANALYSIS OF CIRCUMFERENTIAL
CRACKS IN REACTOR PIPING SYSTEMS

1.0 INTRODUCTION

In 1978, intergranular stress corrosion cracking (IGSCC) was found in a large-diameter (>20 inch) stainless steel pipe in a single boiling water reactor (BWR). This cracking incident and other considerations related to IGSCC prompted the U. S. Nuclear Regulatory Commission (NRC) to form a Pipe Crack Study Group to consider various aspects of IGSCC, including an assessment of the significance of IGSCC in large-diameter stainless steel BWR piping. The Study Group final report (Pef. 1) included a description of a fracture mechanics analysis that was performed to determine the potential for unstable crack extension in large-diameter stainless steel BWR piping that had experienced severe IGSCC. Because the NRC Pipe Crack Study Group report included only a brief summary of the fracture mechanics analysis, this report has been prepared to provide the detailed analytical formulation and calculational procedures used to support the Study Group's conclusions concerning the potential for flaw-induced fracture in large-diameter stainless steel piping.

The IGSCC in BWR piping is found in the heat-affected zone of pipe welds and results from a critical combination of stress, environment, and material sensitization occurring from the welding operation. The cracks initiate at the pipe inner surface and grow radially and circumferentially by the corrosion mechanism. Although many of the stress corrosion cracks are detected during inservice inspection before propagating through the pipe wall, some cracks may actually propagate through the pipe wall. However, should cracks propagate through the pipe wall, leak detection systems are capable of sensing the leaks. Furthermore, even though part-through or through-wall IGSCC may be present, materials used for the piping system, such as Type 304 stainless steel, exhibit such high ductility and toughness that it is very unlikely they will suffer sudden fracture even when relatively large flaws are present. In fact, all of the leaks resulting from stress corrosion cracking have been observed in stainless steel piping that did not fracture.

To provide additional assurance that piping subjected to stress corrosion cracking will leak before breaking, analyses were performed to show that a leaking through-wall crack grows in a stable manner and that it does not cause sudden pipe fracture. In the present study, a fracture mechanics analysis is performed to assess the stability of crack extension in the piping system. The analysis is based on the tearing stability concept and the tearing modulus stability criterion (Ref. 2). The criterion is valid for materials whose failure is characterized by gross yielding of the cross section containing the crack and subsequent plastic stability.

The concept of tearing modulus, T, has been developed on the basis of the J-integral resistance curve and the non-dimensional quantities T_{mat} and T_{appl}. These quantities are defined as

$$T_{mat} = \frac{E}{\sigma_o^2} \frac{dJ_{mat}}{da} \quad (1a)$$

and

$$T_{appl} = \frac{E}{\sigma_o^2} \frac{dJ}{da} \quad (1b)$$

where E is Young's modulus, σ_o is an appropriate flow stress, a is a characteristic flaw size in the stability analysis, J_{mat} is the value of J following the material resistance curve, and J is the applied value of J. The condition of stability of crack growth is given by the following:

$$T_{mat} > T_{appl} \text{ stable} \quad (2a)$$

$$T_{mat} < T_{appl} \text{ unstable} \quad (2b)$$

583 296

~~550 335~~

When Equation 2a is satisfied with a substantial margin, stable crack growth is assured. Rigorous accounts of the concept of T and its applicability are found in References 2 and 3.

In this report, a simplified, conservative stability analysis is made parametrically. In the analysis discussed in Sections 2 and 3, the pipe is treated as a beam whose cracked cross section is subjected to a plastic limit moment. Because segments of the crack on the compressive side may close and carry the compressive load, the analysis is made with and without crack closure. The stability of cracks observed in actual reactor piping is discussed in Section 4.

2.0 METHOD OF ANALYSIS

The tearing stability fracture mechanics analysis is based on the concept of tearing modulus, T, as defined by Equation 1 and requires the knowledge of the applied value of J (or its differential form dJ) in terms of crack size and other geometric details as well as the loading system configuration and stiffness.

To facilitate the analysis, the pipe is treated as a beam subjected to bending and axial loads. To ensure a conservative analysis, the following conditions are imposed:

1. The cross section containing a crack is fully yielded.
2. The material is assumed to be perfectly plastic (or elastic perfectly plastic with large deformations).

That is, the cracked section of the pipe is subjected to the plastic limit moment, M_p.

With the given conditions, it is convenient to use the following definition of J (Ref. 4):

583 297

~~550 336~~

$$J = -\int_{0}^{M} \left(\frac{\partial M}{\partial A}\right)_{\phi} d\phi \tag{3}$$

where A is the crack area, M is a bending moment applied on a cracked body, and ϕ is the corresponding angle of rotation. When perfectly plastic behavior is assumed and the limit moment is reached, Equation 3 is rewritten (see Figure 1) as

$$J = -\frac{\partial M_p}{\partial A}\phi \quad \text{or} \quad dJ = -\frac{\partial M_p}{\partial A}d\phi \tag{4}$$

Note that the axial force is normally a built-in load, such as internal pressure, is independent of flaw size, and is not usually expected to be large enough to cause gross yielding of the net section. The influence of the axial force on the J value is taken into account, in effect, by changing the location of neutral axis and the limit moment, M_p. Thus, Equation 4 will provide a reasonable approximation of J, including the effect of axial loads. If J is known as a function of crack size and other variables, then the stability analysis may be performed for each specified loading system.

The geometry of the cracked section of the pipe is assumed to be as shown in Figure 2. That is, the section contains an internal circumferential crack in addition to a through-wall crack. The following notation is used in the present analysis (see Figure 2):

R = radius of the pipe measured to the middle of the wall
t = thickness of the pipe wall
2θ = angle contained by the through-wall crack
a = depth of the circumferential crack
σ_o = flow stress
P = axial force

In addition, it is convenient to introduce the following nondimensional quantities:

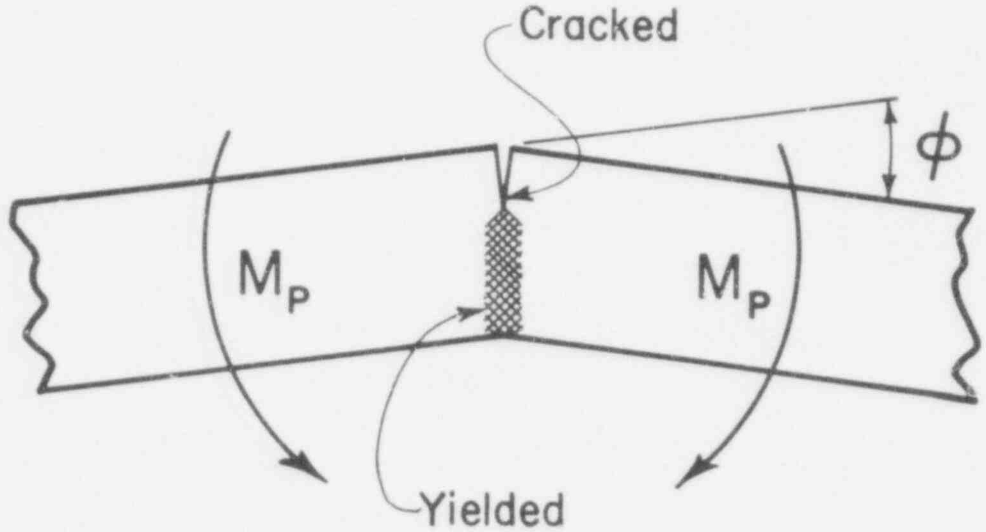

Figure 1. Limit moment, M_p, and angle of rotation, ϕ.

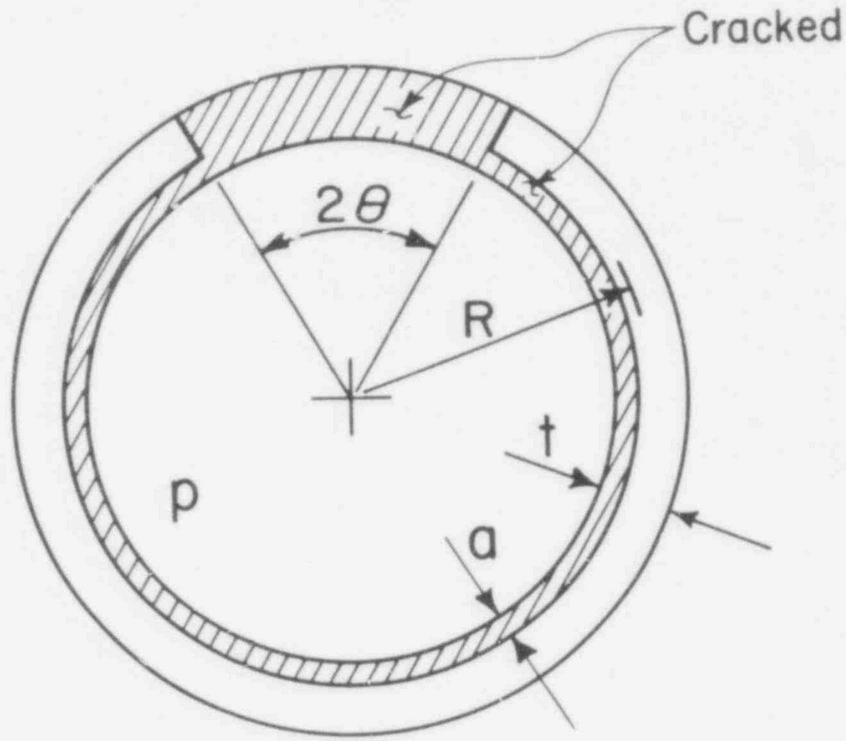

Figure 2. Cracked section of pipe.

550 339

583 300

$$\bar{a} = \frac{a}{t} \tag{5a}$$

$$\bar{P} = \frac{P}{(2\pi Rt)\,\sigma_o} \tag{5b}$$

Because a part of the crack located on the compressive side may close and carry some compressive load, the analysis considers the two extreme cases:

1. No crack closure occurs on the compressive side, or
2. The crack closes completely on the compressive side and carries compressive load.

These two situations are shown in Figure 3.

When examining Figure 3, it can be seen that the location of neutral axis defined by angle α, the limit moment, M_p, and the J value, etc., are functions of four variables (that is, t/R, θ, $\bar{a}$, and $\bar{P}$) and depend on the closure condition 1 or 2. For simplicity, we may now assume that the pipe is a thin-walled cylinder; that is,

$$t/R \ll 1 \tag{6}$$

Under this assumption, one parameter, t/R, is eliminated from the analysis. Also, when the axial force, P, results from an internal pressure, p, is related to p by

$$\bar{P} = \frac{1}{2}\left(\frac{R}{t}\right)\left(\frac{p}{\sigma_o}\right) \tag{7}$$

The expressions for the location of neutral axis, α, the limit moment, M_p, and the J value are given in the following sections in terms of the remaining three parameters (θ, $\bar{a}$, and $\bar{P}$) for both closure conditions 1 and 2. A simplified crack instability analysis follows.

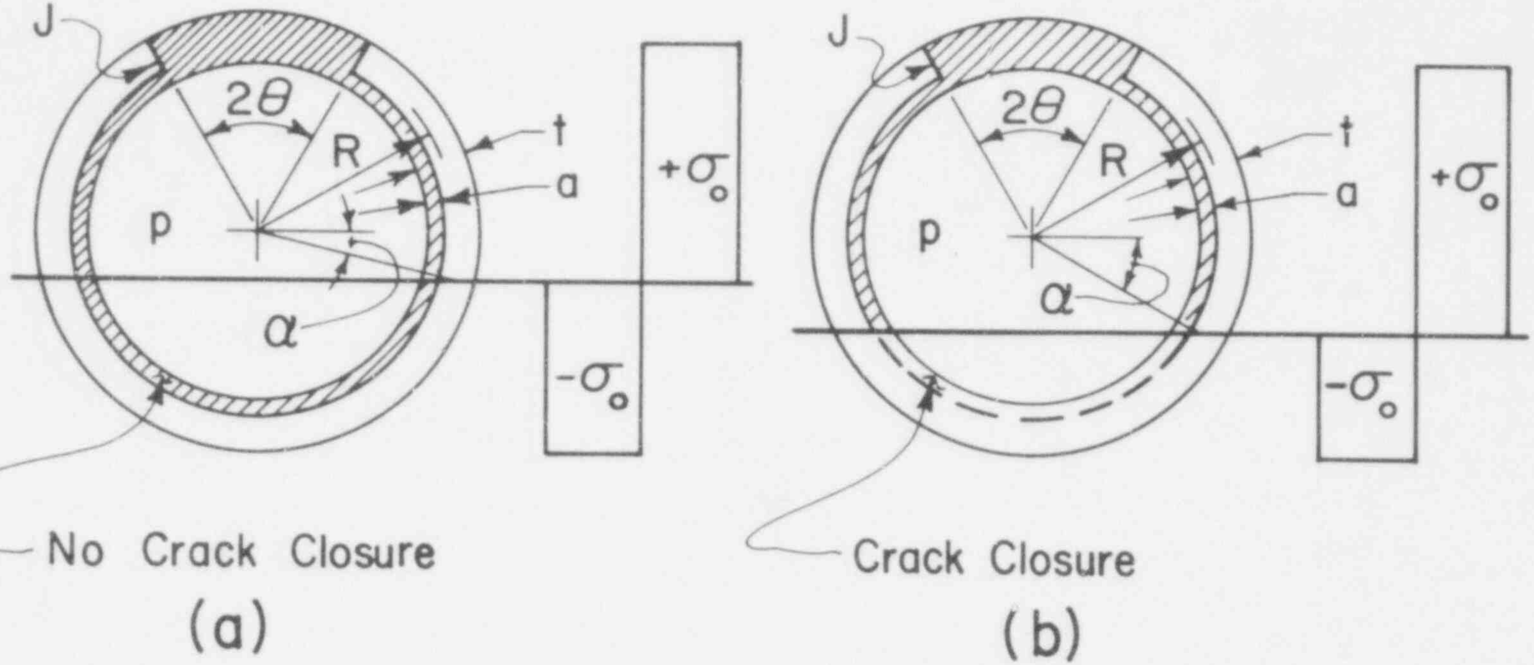

Figure 3. Location of neutral axis, α.

2.1 Location of the Neutral Axis

The location of the neutral axis is defined by an angle α as shown in in Figure 3. In this case, $\alpha = \alpha(\theta,\bar{a},\bar{P})$ is readily written as follows:

Without crack closure (see Figure 3a):

$$\alpha = \frac{1}{2}\theta + \frac{\pi}{2}\frac{\bar{P}}{1-\bar{a}} \tag{8a}$$

With crack closure (see Figure 3b):

$$\alpha = \frac{1-\bar{a}}{2-\bar{a}}\theta + \frac{\pi}{2-\bar{a}}\left(\bar{P} + \frac{\bar{a}}{2}\right) \tag{8b}$$

2.2 Plastic Limit Moment

Having located the neutral axis, the limit moment, M_p, is also readily calculated by geometric considerations. It is convenient to normalize M_p in the form

$$M_p = 4\,\sigma_o\,R^2 t\,\bar{M}_p(\theta,\bar{a},\bar{P}) \tag{9}$$

Note that $4\sigma_o R^2 t$ is the limit of the gross section of the pipe ($\theta = \bar{a} = o$) under pure bending ($\bar{P} = o$). $\bar{M}_p$ is a nondimensional representation of the limit moment, which is given by the following:

Without crack closure:

$$\bar{M}_p = (1-\bar{a})\,(\cos\alpha - \frac{1}{2}\sin\theta) + \frac{\pi}{2}\bar{P}\sin\alpha \tag{10a}$$

where α is given by Equation 8a.

583 303

~~550~~ 342

With crack closure:

$$\bar{M}_p = (1-\bar{a}) \left(\frac{1 - \frac{1}{2}\bar{a}}{1-\bar{a}} \cos\alpha - \frac{1}{2}\sin\theta \right) + \frac{\pi}{2}\bar{P}\sin\alpha \quad (10b)$$

where α is given by Equation 8b.

The numerical values of $\bar{M}_p$ are plotted against θ in Figures 4 and 5 for various values of each parameter and for both cases with and without crack closure.

The limit moment, M_p, increases slightly as the axial force, P, increases with other variables unchanged. However, the magnitude of bending moment, which can be externally applied on the cracked section, decreases due to the axial force. To obtain the applied value of J, the total magnitude, M_p, is used in Equation 4.

2.3 Expression of J

Because we are interested in the stability of the through-wall crack extending in the circumferential direction, J should be calculated along the radial edge of the crack. Referring to Figure 2, the increment of crack area, dA, is given by

$$dA = 2Rt(1-\bar{a})\, d\theta \quad (11)$$

Substituting this into Equation 4 and combining with Equation 9, J is calculated as follows:

$$J = -\frac{2\sigma_o R}{1-\bar{a}} \cdot \frac{\partial\bar{M}_p}{\partial\theta} \cdot \phi \quad (12)$$

583 304

~~550 343~~

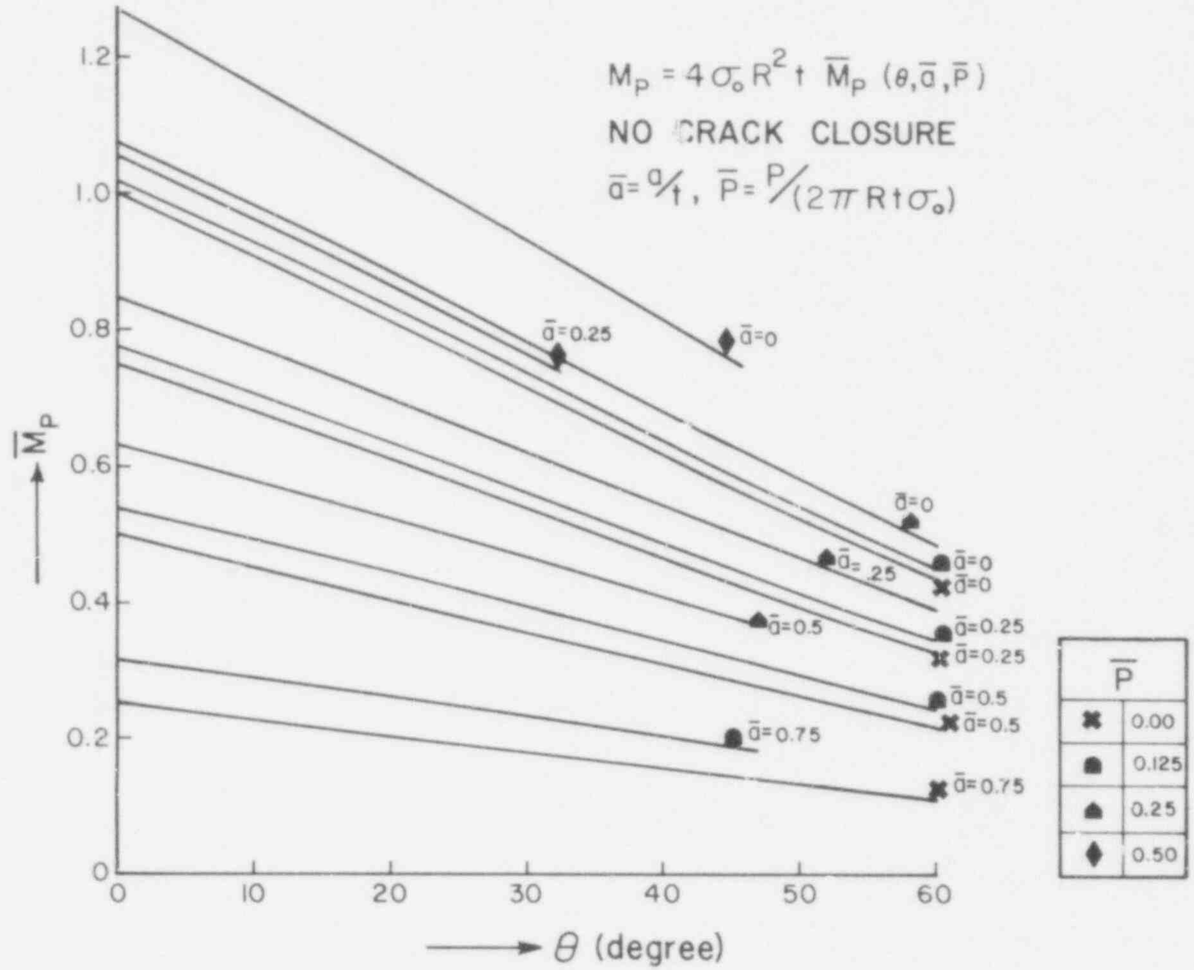

Figure 4. M_p versus θ, without crack closure.

550 344

583 305

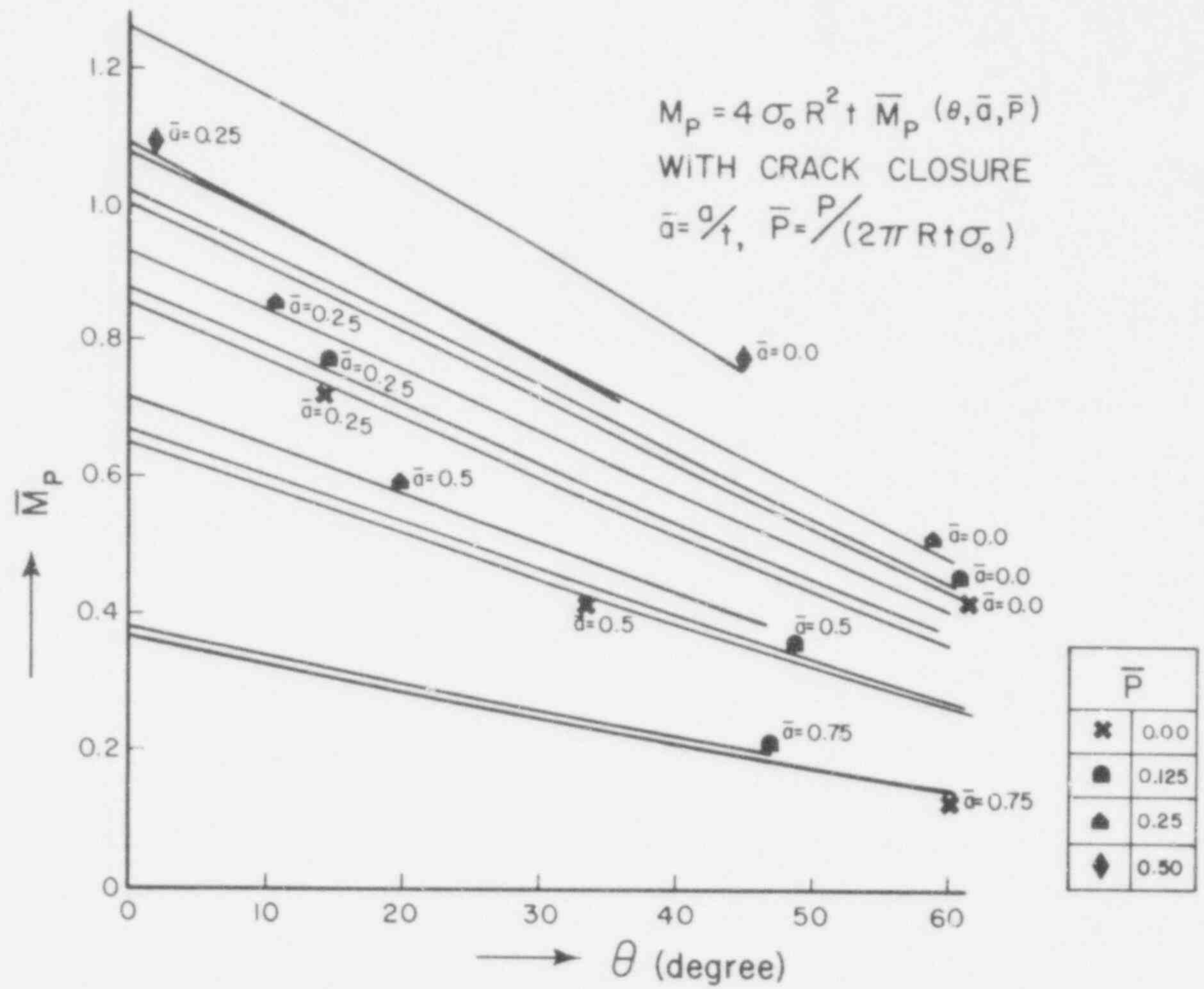

Figure 5. M_p versus θ, with crack closure.

J is conveniently normalized in the form

$$J = (\sigma_o R)\,\bar{J} = (\sigma_o R)\, F_J\,(\theta,\bar{a},\bar{P}) \cdot \phi \tag{13}$$

where $\bar{J} = F_J\,(\theta,\bar{a},\bar{P}) \cdot \phi$ is a nondimensional representation of J and

$$F_J\,(\theta,\bar{a},\bar{P}) = -\,\frac{2}{1-\bar{a}}\,\frac{\partial \bar{M}_p}{\partial \theta} \tag{14}$$

Combining Equations 8, 10, and 14, $F_J\,(\theta,\bar{a},\bar{P})$ is written in the following simple form.

Without crack closure:

$$F_J = \sin\alpha + \cos\theta - \frac{\pi}{2}\,\frac{\bar{P}}{1-\bar{a}}\cos\alpha \tag{15a}$$

With crack closure:

$$F_J = \sin\alpha + \cos\theta - \frac{\pi}{2}\,\frac{\bar{P}}{1-\frac{\bar{a}}{2}}\cos\alpha \tag{15b}$$

where α is given by Equations 8a and 8b respectively.

The numerical values of F_J are shown in Figures 6 and 7 for various values of the parameters.

The preceding analysis of J and the subsequent stability analysis are readily generalized for a cracked beam with an arbitrary cross-section subjected to the limit moment (Figure 8). Note that J is always given in the form

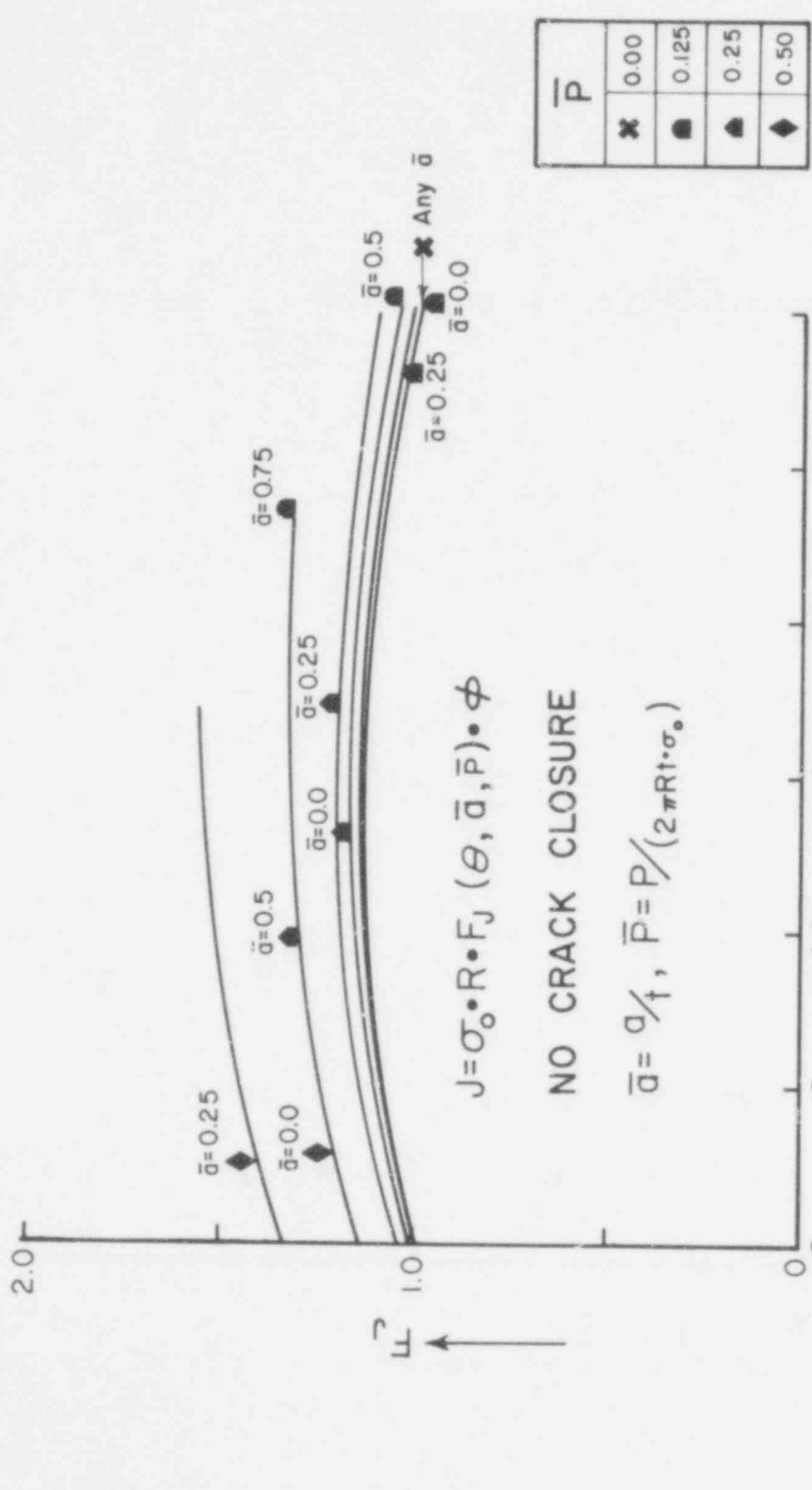

Figure 6. F_J versus θ, without crack closure.

583 308
~~550 347~~

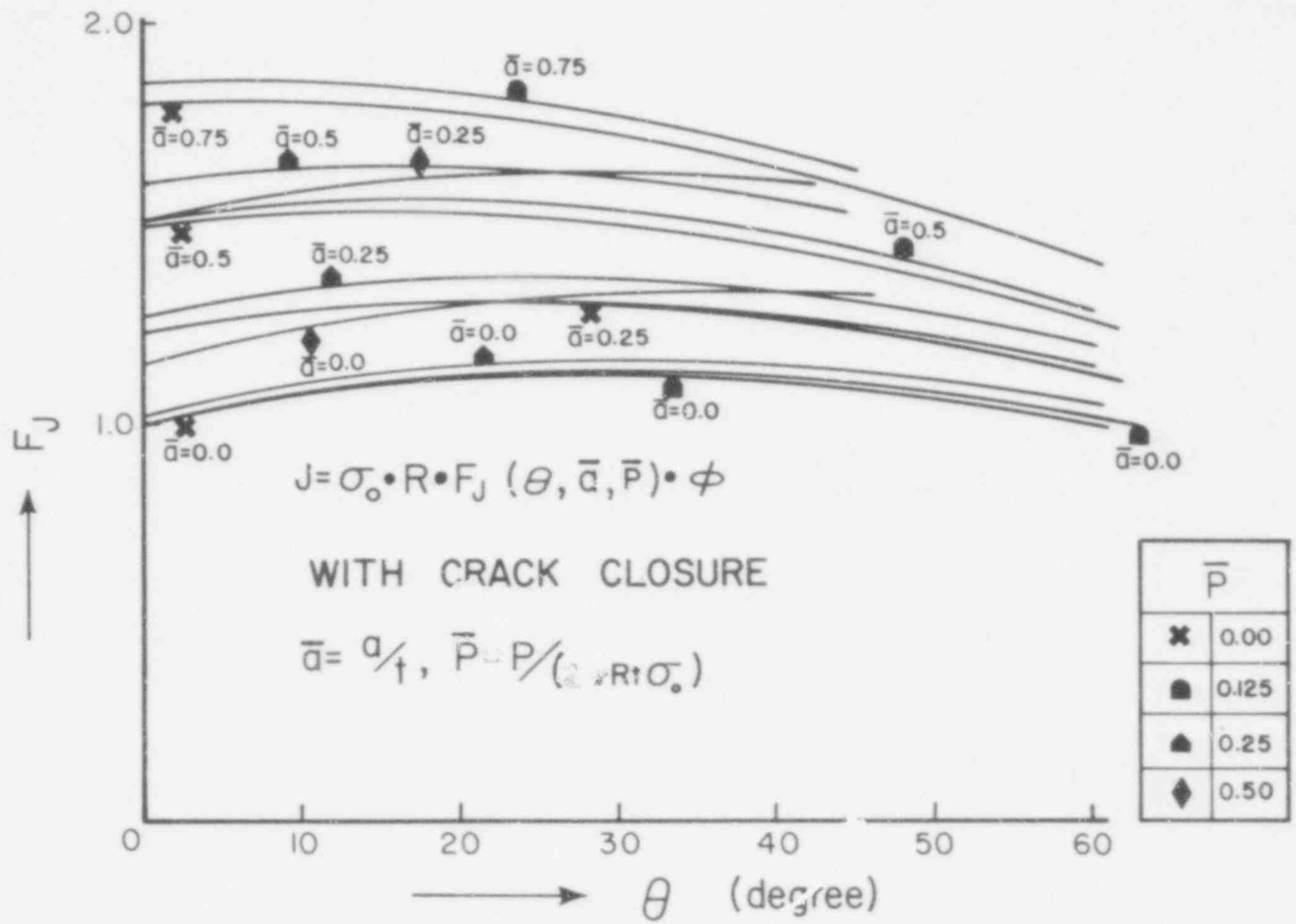

Figure 7. F_J versus θ, wit crack closure.

583 309

~~550~~ 348

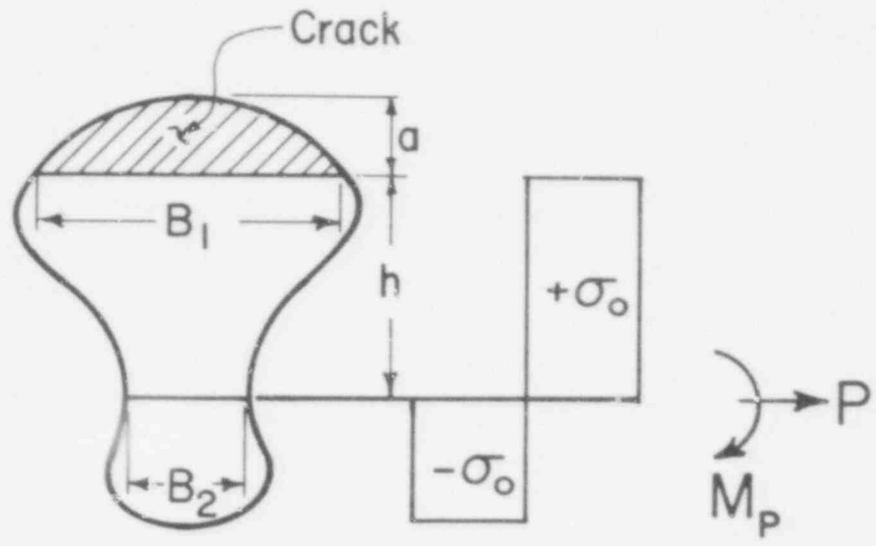

$$J = -\frac{\partial M_p}{B_1\, \partial a}\,\phi = \sigma_o\left(h - \frac{1}{2}\frac{A_p}{B_2}\right)\phi$$

$$A_p = \frac{P}{\sigma_o}$$

Figure 8. Cracked beam with arbitrary cross section.

583 310

~~550 349~~

$$J = \left(\sigma_o h - \frac{1}{2} \frac{P}{B}\right)\phi \qquad (16a)$$

or

$$J = \sigma_o \left(h - \frac{1}{2} \frac{A_p}{B}\right)\phi \qquad (16b)$$

where, referring to Figure 8,

- h = vertical distance from the neutral axis to the crack edge
- B = width of the beam at the location of neutral axis
- P = axial force
- A_p = area given by P/σ_o

Alternately, the expressions of J given by Equations 13 and 15 can also be obtained from Equation 16.

3.0 SIMPLIFIED INSTABILITY ANALYSIS

The previously discussed data allows a conservatively simplified instability analysis of crack extension in the piping system to be made. The analysis uses the procedure similar to that discussed in Reference 2. That is, by referring to Figure 9, when a rotation $\tilde{\phi}$ is imposed at the fixed ends of the beam, $\tilde{\phi}$ is written in the following form considering separately the elastic part, ϕ_{el}, and the plastic part, ϕ_{pl}:

$$\tilde{\phi} = \phi_{el} + \phi_{pl} \qquad (17)$$

The total rotation $\tilde{\phi}$ remains constant during the examination of stability.

583 311

~~550 350~~

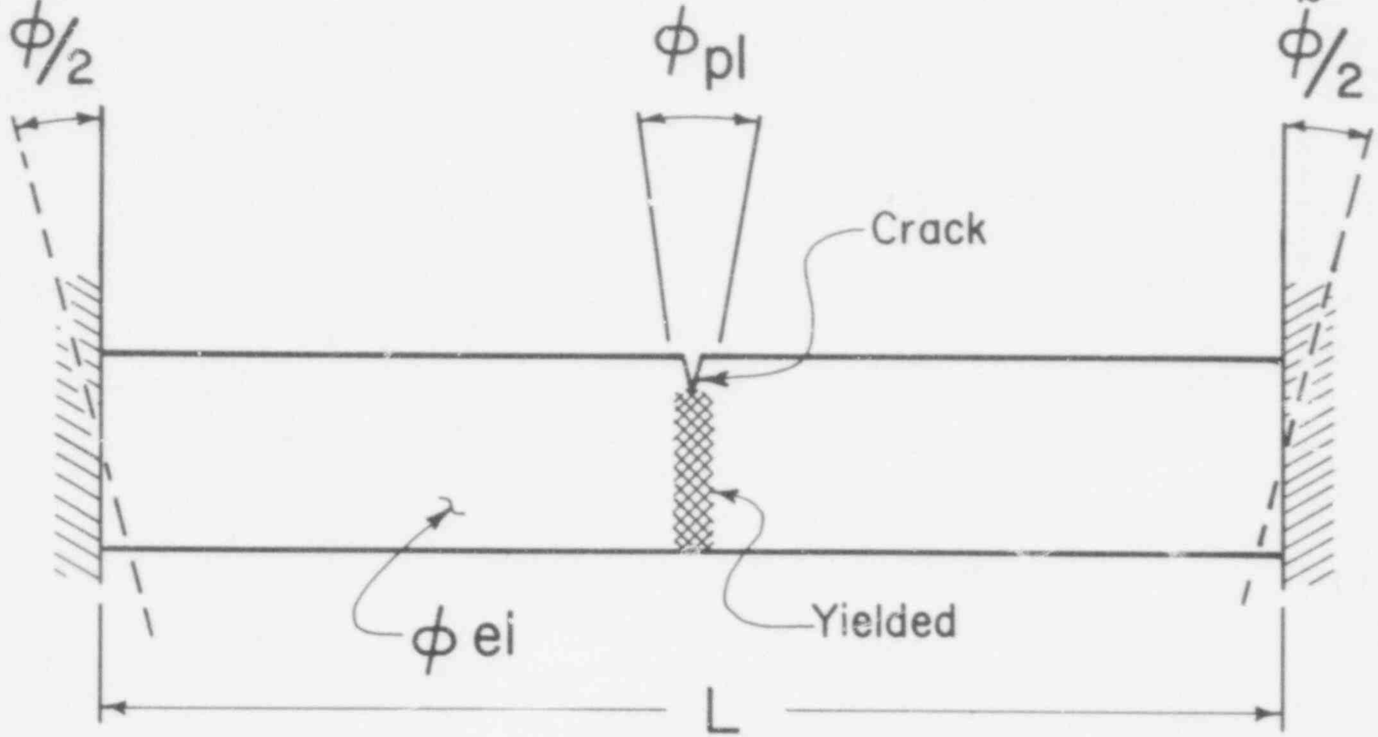

Figure 9. Fixed beam under uniform bending, $\tilde{\phi}$ = constant.

583 312

~~550 351~~

$$d\widetilde{\phi} = d\phi_{el} + d\phi_{pl} = 0 \tag{18}$$

The elastic part of rotation, ϕ_{el}, has the form

$$\phi_{el} = \frac{L}{\rho} = \frac{ML}{EI} \tag{19}$$

where $M = M_p$ (limit moment, Equation 9) and $I = \pi R^3 t$. The plastic part of the rotation, ϕ_{pl}, is from Equation 13:

$$\phi_{pl} = \frac{J}{\sigma_o R} \cdot \frac{1}{F_J} \tag{20}$$

where F_J is given by Equation 15.

Because we are interested in the through-wall crack as it extends in the θ direction, from Equation 19

$$d\phi_{el} = \frac{\partial M_p}{\partial \theta} \frac{L}{EI} \; d\theta \tag{21}$$

By combining Equations 9 and 14, $d\phi_{el}$ is written in the form

$$d\phi_{el} = - \frac{2}{\pi} \; \frac{\sigma_o}{E} \; (1-\bar{a}) \; \left(\frac{L}{R}\right) F_J(\theta,\bar{a},\bar{P}) \; d\theta \tag{22}$$

583 313

~~550~~ 352

Also, from Equation 20, noting that both J and F_J contain θ,

$$d\phi_{pl} = \frac{\partial\phi_{pl}}{\partial J} \; dJ + \frac{\partial\phi_{pl}}{\partial F_J} \; dF_J \tag{23}$$

For convenience, Equation 23 can also be written in the following form:

$$d\phi_{pl} = \frac{1}{\sigma_o R F_J} \; dJ + \frac{J}{\sigma_o R}\left(-\,\frac{1}{F_J{}^2}\right)\frac{\partial F_J}{\partial\theta}\, d\theta \tag{24}$$

By substituting Equations 22 and 24 into Equation 18 and noting that the crack increment in the θ direction is $Rd\theta$, we have

$$\frac{dJ}{Rd\theta} \cdot \frac{E}{\sigma_o{}^2} = F_1(\theta,\bar{a},\bar{P}) \cdot \frac{L}{R} + F_2\,(\theta,\bar{a},\bar{P}) \cdot \frac{JE}{\sigma_o{}^2 R} \tag{25}$$

where F_1 and F_2 are related to F_J as follows:

$$F_1 = \frac{2}{\pi}\,(1-\bar{a})\;F_J{}^2 \tag{26}$$

and

$$F_2 = \frac{1}{F_J} \cdot \frac{\partial F_J}{\partial\theta} \tag{27}$$

Thus, T_{appl} in the instability condition (see Equation 2b) is given by

583 314

~~550 353~~

$$T_{appl} = F_1(\theta,\bar{a},\bar{\beta})\,\frac{L}{R} + F_2\,(\theta,\bar{a},\bar{\beta})\;\frac{JE}{\sigma_o{}^2 R} \tag{28}$$

From Equations 15, 26, and 27, F_1 and F_2 are written in the following form:

With no crack closure:

$$F_1 = \frac{2}{\pi}\,(1-\bar{a})\;F_J{}^2 \tag{29}$$

and

$$F_2 = \frac{1}{2}\;\frac{1}{F_J}\left(\cos\alpha - 2\,\sin\theta + \frac{\pi}{2}\;\frac{\bar{\beta}}{1-\bar{a}}\;\sin\alpha\right) \tag{30}$$

where α and F_J are given by Equations 7a and 15a, respectively.

With crack closure:

$$F_1 = \frac{2}{\pi}\,(1-\bar{a})\;F_J{}^2 \tag{31}$$

and

$$F_2 = \frac{1}{2}\;\frac{1}{F_J}\;\;\frac{1-\bar{a}}{1-\frac{\bar{a}}{2}}\left(\cos\alpha - \frac{2-\bar{a}}{1-\bar{a}}\,\sin\theta + \frac{\pi}{2}\;\frac{\bar{\beta}}{1-\frac{\bar{a}}{2}}\,\sin\alpha\right) \tag{32}$$

where α and F_J are given by Equations 8b and 15b, respectively.

The numerical values of F_1 and F_2 are presented against θ in Figures 10 through 13, for various values of parameters and conditions with and without crack closure.

583 315

~~550 354~~

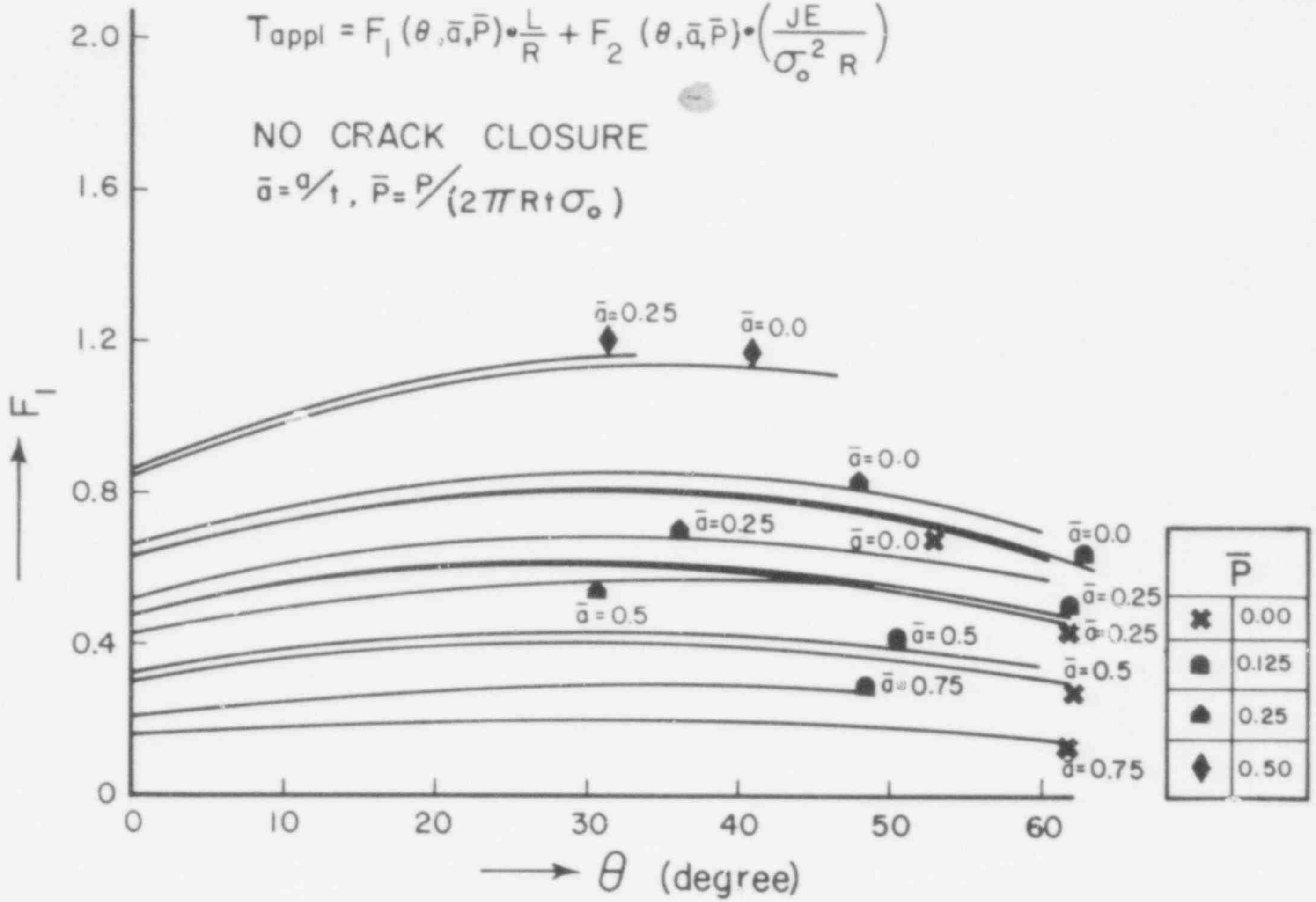

Figure 10. F_1 versus θ, without crack closure.

583 316

~~550 355~~

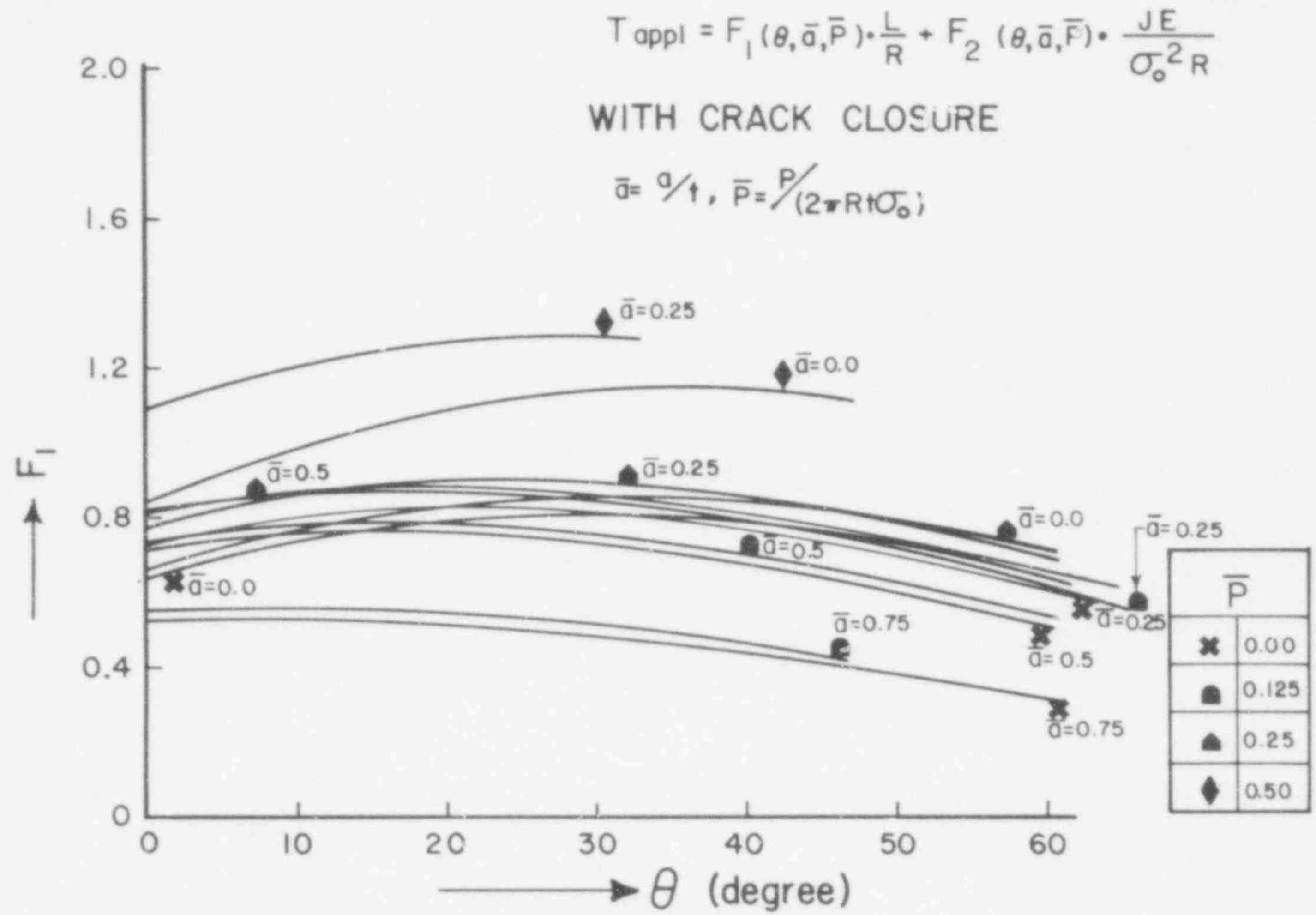

Figure 11. F_1 versus θ, with crack closure.

583 317

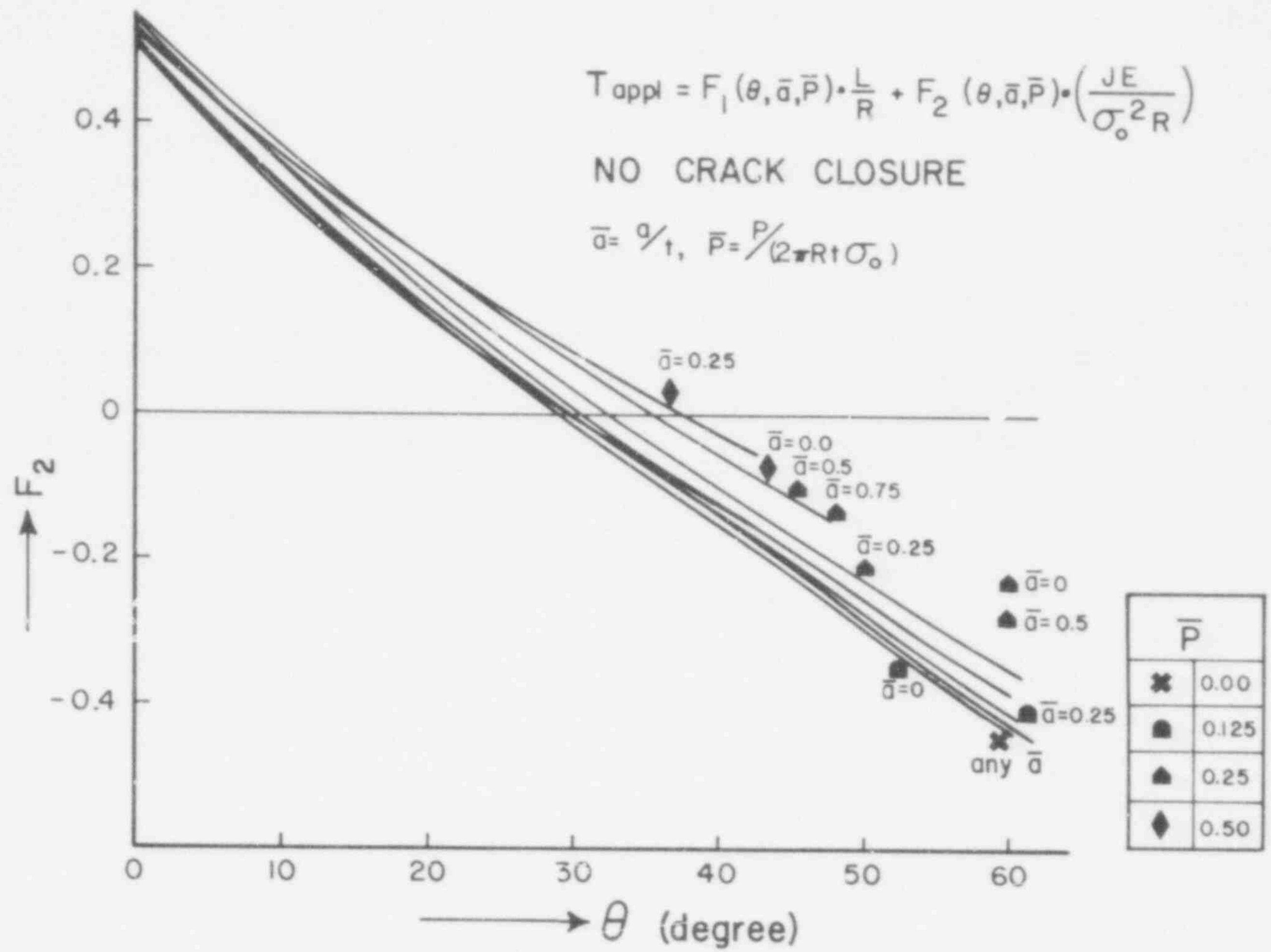

Figure 12. F_2 versus θ, without crack closure.

583 318

~~550~~ 357

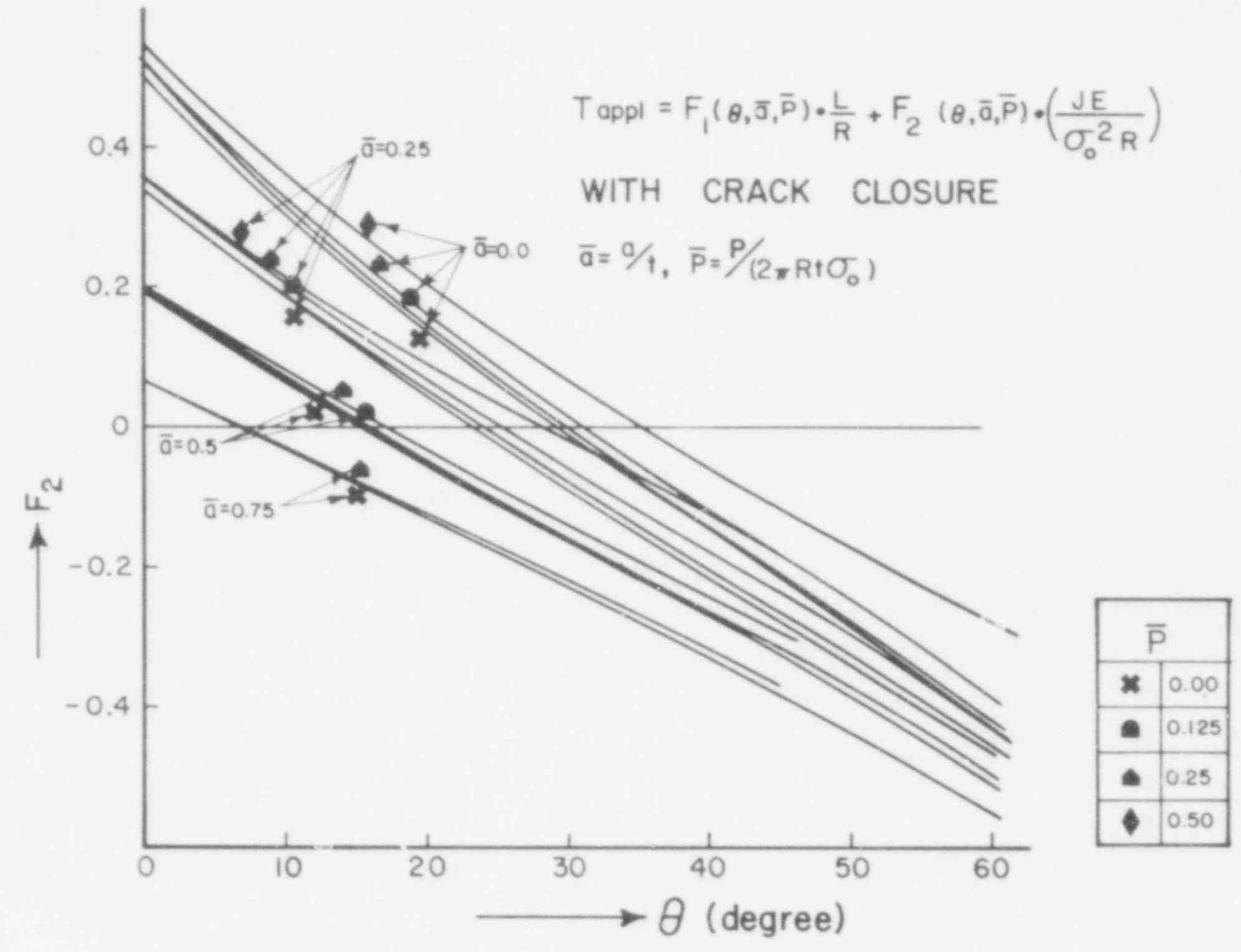

Figure 13. F_2 versus θ, with crack closure.

Considering that the first term on the right-hand side of Equation 28, $F_1 \cdot (L/R)$, results from relaxation of the elastic deformation of the beam (or pipe) during the crack increment, we may reasonably expect that the uniform bending condition imposed in the present analysis is more severe than other loading conditions or pipe geometry provided the length of pipe, L, between the supports is equal. For example, consider a simply supported pipe subjected to a concentrate load that causes the maximum bending moment equal to M_p at the cracked section as shown in Figure 14. When we impose the condition that total vertical displacement at the load point remains constant ($d\Delta = 0$) during the instability analysis, T_{appl} is given by

$$T_{appl} = \frac{1}{3} F_1(\theta,\bar{a},\bar{P}) \frac{L}{R} + F_2(\theta,\bar{a},\bar{P}) \frac{JE}{\sigma_o^2 R} \qquad (33)$$

where F_1 and F_2 are the same functions as in Equation 28. Note that the change in loading condition results in the change in the coefficient of the first term and does not change the second term. Thus, T_{appl} given by Equation 28 is expected to provide the upper bound of the T_{appl} value in real structural situations.

4.0 APPLICATION

Consider a 28-inch BWR stainless steel recirculation outlet line that might contain a large intergranular stress corrosion crack in its wall. This line was selected because it can have the largest possible coolant loss should a pipe rupture occur. The geometry of the cracked section is as follows (refer to Figure 2):

583 320
~~550 359~~

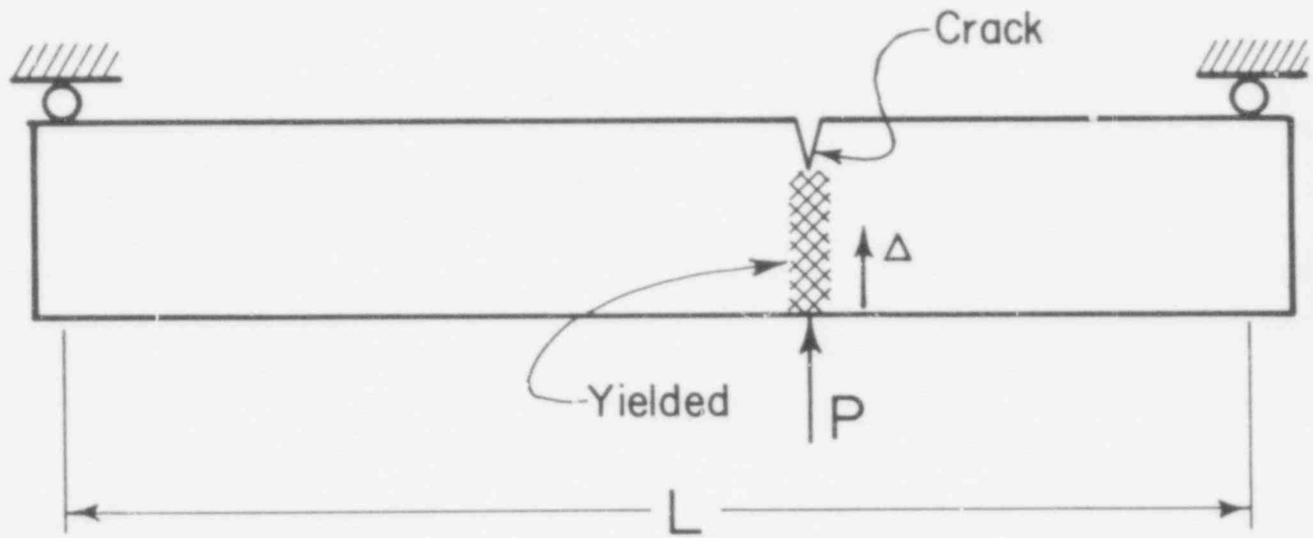

Figure 14. Simply supported beam, Δ = constant.

$R = 14$ in.

$t = 1.5$ in.

$2\theta \simeq 100$ degree (for example)

$\bar{a} = a/t \simeq 0.75$ (for example)

The applied pipe loading is assumed to be the BWR design pressure and a bending moment sufficient to produce a fully plastic bending moment in the remaining ligament of the cracked pipe section. The assumed bending load necessary to produce a fully plastic moment in the cracked section corresponds to conservative pipe deflections and is significantly larger than the ASME Code design allowable for normal operation and anticipated transients. The flow stress, σ_o, is assumed to be 50 ksi accounting for hardening. Then, from Equation 5, the value of $\bar{P}$ is approximately 0.1.

For these values of variables, the functions F_1 and F_2 in Equations 29 through 32 are read from Figures 10 through 13. That is,

Without crack closure (Figures 10 and 12):

$F_1 \simeq 0.24$

$F_2 \simeq -0.28$

With crack closure (Figures 11 and 13):

$F_1 \simeq 0.4$

$F_2 \simeq -0.44$

Therefore, the T_{appl} is conservatively given by

$$T_{appl} = 0.4 \left(\frac{L}{R}\right) + (-0.28) \quad \frac{JE}{\sigma_o^2 R} \tag{34}$$

583 322

061

Using an experimental crack resistance curve for stainless steel (Ref. 5) and assuming a significant crack extension, it is seen that the J value is approximately 4000 in.-lb/in.^{2}. Taking J = 4000 in.-lb/in.^{2} for conservativeness,

$$T_{appl} = 0.4 \left(\frac{L}{14}\right) - 1.0$$

The value of T_{mat} for stainless steel is normally larger than 200 (Ref. 5). Assuming that T_{mat} = 200, Equation 2 requires L ≈ 600 ft for instability.

It should be noted from Figures 10 through 13 that, for the range of variables considered in the present study,

$$T_{appl} < 1.3 \frac{L}{R} + 0.5 \frac{JE}{\sigma_o^2 R}$$

Thus, the instability criterion, Equation 2b, always requires a very large value of L/R for instability.

Because values of L/R for BWR piping systems are generally relatively small compared to the calculated values for instability, unstable crack extension will probably not occur in BWR stainless steel piping systems designed in accordance with the ASME Code, even though severe IGSSC may be present.

5.0 SUMMARY

The high ductility and toughness of the stainless steel reactor system piping have made it virtually certain not to experience unstable crack extension. The present study has attempted to provide theoretical assurance that the piping system will not experience unstable crack extension, even if severe intergranular stress corrosion cracking should occur.

The analysis is based on the tearing instability concept and the associated tearing modulus stability criterion. A conservative analysis successfully demonstrated that sudden fracture would probably not occur from circumferential IGSCC in stainless steel piping systems designed in accordance with the ASME Code, provided that values of L/R are less than approximately 200. Because values of L/R in BWR stainless steel piping systems range between 20 and 30, unstable crack extension will probably not occur, even though severe IGSCC may exist. Should stainless steel piping have values of L/R beyond 200, a more detailed analysis would be necessary to demonstrate crack stability.

6.0 REFERENCES

1. U. S. Nuclear Regulatory Commission, "Investigation and Evaluation of Stress-Corrosion Cracking in Piping of Light Water Reactor Plants," USNRC Report NUREG-0531, February 1979. Available for purchase from the National Technical Information Service, Springfield, Virginia 22161.
2. P. C. Paris, et al., "A Treatment of the Subject of Tearing Instability," USNRC Report NUREG-0311, August 1977. (See also ASTM STP 668, April 1979. pp. 5-36). Available for purchase from the National Technical Information Service, Springfield, Virginia 22161. (See also public or technical libraries.)
3. J. W. Hutchinson and P. C. Paris, "Stability Analysis of J-Controlled Crack Growth," ASTM STP 668, April 1979, pp. 37-64. Available from public technical libraries.
4. J. R. Rice, "Mathematical Analysis in the Mechanics of Fracture," in Fracture, Vol. 2 (Academic Press, Inc., 111 Fifth Avenue, New York, New York 10003, 1968), pp. 192-311. Available from publisher.
5. W. H. Bamford and A. J. Bush, "Fracture Behavior of Stainless Steel," ASTM STP 668, April 1979, pp. 553-557. Available from public or technical libraries.

583 324

~~550 362~~

NRC FORM 335 (7-77)

U.S. NUCLEAR REGULATORY COMMISSION

BIBLIOGRAPHIC DATA SHEET

1. REPORT NUMBER (Assigned by DDC): NUREG/CR-0838

4. TITLE AND SUBTITLE (Add Volume No., if appropriate)
A Stability Analysis of Circumferential Cracks for Reactor Piping Systems

2. (Leave blank)

3. RECIPIENT'S ACCESSION NO.

7. AUTHOR(S)
H. Tada, P. Paris, R. Gamble

5. DATE REPORT COMPLETED
MONTH: February YEAR: 1979

9. PERFORMING ORGANIZATION NAME AND MAILING ADDRESS (Include Zip Code)
Center for Fracture Mechanics
Washington University
Campus Box 1124
St. Louis, Missouri 63130

DATE REPORT ISSUED
MONTH | YEAR

6. (Leave blank)

8. (Leave blank)

12. SPONSORING ORGANIZATION NAME AND MAILING ADDRESS (Include Zip Code)
U. S. Nuclear Regulatory Commission
Office of Nuclear Reactor Regulation
Washington, D. C. 20555

10. PROJECT/TASK/WORK UNIT NO.

11. CONTRACT NO.

13. TYPE OF REPORT
Technical Report

PERIOD COVERED (Inclusive dates)

15. SUPPLEMENTARY NOTES

14. (Leave blank)

16. ABSTRACT (200 words or less)

A simplified fracture mechanics analysis was performed to determine the potential for unstable tearing in boiling water reactor (BWR) stainless steel piping systems, which have severe intergranular stress corrosion cracking (IGSCC). The fracture analysis was based on the tearing stability concept and associated tearing modulus stability criterion.

The results from this study indicate that unstable crack extension would probably not occur in BWR stainless steel piping systems designed in accordance with the ASME Code even though severe IGSCC may be present. The analysis indicated that stainless steel piping with severe IGSCC could experience unstable fracture if the piping length to radius ratio (L/R) was very large (approximately 200). Since the values of L/R for BWR stainless steel piping systems are generally an ordc of magnitude less than this, largc margins against unstable fracture are assured for these systems.

17. KEY WORDS AND DOCUMENT ANALYSIS

17a. DESCRIPTORS

17b. IDENTIFIERS/OPEN-ENDED TERMS

18. AVAILABILITY STATEMENT
Unlimited Availability

19. SECURITY CLASS (This report)

21. NO. OF PAGES

20. SECURITY CLASS (This page)

22. PRICE
$

NRC FORM 335 (7-77)

583 325 ~~550 363~~